



The Compact Muon Solenoid Experiment

CMS Note

Mailing address: CMS CERN, CH-1211 GENEVA23, Switzerland



February 9, 1999

Design of the Track Correlator

for the DTBX Trigger

R. Martinelli, A.J. Ponte Sancho¹, P. Zotto²

Sezione I.N.F.N. di Padova, Italy

Abstract

The fully reviewed design of the Track Correlator (TRACO) developed for the muon barrel drift tubes first level trigger is presented.

Details of the project and a study of the expected performance of the device, based on a full GEANT simulation using the CMS113 version of the detector, are given.

¹ Now at Universidade do Algarve, UCEH, Gambelas, Faro, Portugal

² Also at Dip. di Fisica del Politecnico di Milano, Italy

1. Introduction

The proposed baseline of the DTBX chamber trigger is a multistage scheme.

The front-end trigger device is called Bunch and Track Identifier (BTI)^[1]: it performs a rough track reconstruction and uniquely identifies the parent bunch crossing of the candidate track by means of a generalized mean-timer technique. First prototypes were already produced.

The BTI is followed in the electronics chain by a Track Correlator (TRACO) that is required to associate portions of tracks in the same chamber relating predefined groups of BTIs among them.

A third device, called Trigger Server^[2], performs the track selection within a full chamber and forwards information to the Muon Regional Trigger^[3], that finally extracts the track candidate transverse momentum.

This note will describe the final TRACO design and provide information about its expected performance.

2. Short Description of BTI

The Bunch and Track Identifier was studied to work on each groups of four layers of staggered drift tubes called Super Layers (SL), aiming to the identification of the tracks giving a signal in at least three of the planes. We quickly recall the basic description of the device: any other detail can be found in Reference 4.

Each BTI is connected to nine wires allocated as shown in Figure 1.

The parameters computed from the BTI are the angular k-parameter $k = h \tan \psi$ (the track direction) and the crossing position, computed in the SL central plane. The geometrical quantities involved are shown in Figure 1: ψ is the angle of the track with respect to the normal to the chamber and $h = 1.3mm$ is the distance between the wire planes.

These parameters are evaluated by means of a generalized mean-timer technique: this

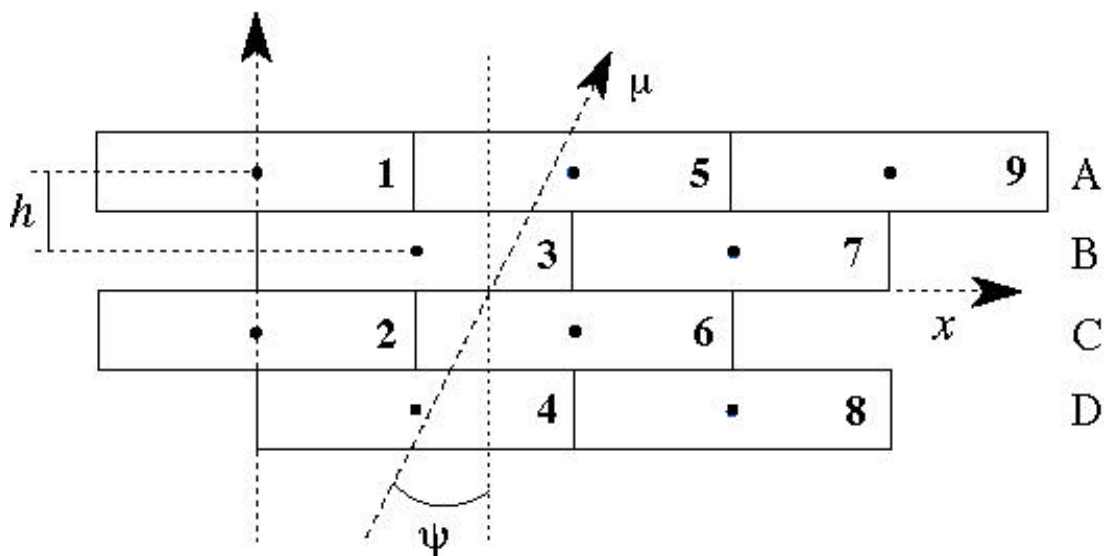


Figure 1 - BTI layout showing channels allocation.

method is a search inside a BTI for the alignments of the recorded hits belonging to a track. If there is an alignment of four hits the signal is marked as High Quality Trigger (HTRG), while if it is due to the alignment of only three hits, it is marked as Low Quality Trigger (LTRG).

The alignment occurs with fixed delay with respect to the parent bunch crossing time, thus permitting its identification. The total latency of the BTI is determined by the maximum drift-time to the wires, T_{MAX} , plus 4 clock cycles needed for input signal synchronization and BTI calculations. For a nominal drift velocity of $50 \mu\text{m/ns}$ the delay of the TRG signal with respect to the parent interaction is therefore 20 bunch crossings.

The BTI trigger algorithm actually generates HTRGs and LTRGs when the computed k-parameters of any of the predefined patterns of wires are equal within the programmed tolerance. The definition and the full list of the preloaded patterns is available in Reference 4.

Position and angular resolution of the device depend on the drift velocity and on the sampling frequency of the device. For a nominal drift velocity of $50 \mu\text{m/ns}$ and a sampling frequency of 40 MHz, the angle is measured with a resolution better than 60mrad, while the position is measured with a resolution of 1.25mm. The angular resolution is track pattern dependent and is generally worse for LTRGs.

Using the current geometric parameters of the chamber, as described in version 113 of the CMS detector software, the angular acceptance is nominally $\psi_{MAX} = \pm 55^\circ$.

Each SL is equipped with one BTI every four wires and the BTIs are overlapped by five wires assuring that every track, with angle within the maximum acceptance range, is fully contained in at least one BTI.

K-parameter and position of the track as measured from the corresponding equations, coded in 6 bits, and one trigger quality bit, marking HTRG or LTRG (H/L), are transmitted to the TRACO on the BTI track-data bus.

Only one track per bunch crossing per BTI is forwarded to the TRACO.

3. Track Correlator layout

The DTBX chamber is composed of two SL in the CMS transverse plane (ϕ view) and one SL in the longitudinal one (θ view). Each SL is equipped with BTIs.

The TRACO is a processor that interconnects the two SL of the transverse plane. It receives the information from the BTI devices connected to it and tries to find the couple of BTI track segments that fits the best track, linking the inner layer candidates to the outer layer ones.

The introduction of this device is necessary since the BTI is intrinsically a noisy device and therefore a local preselection and a quality certification of the BTI triggers is required. Furthermore the number of BTIs per chamber is around few hundreds and it is not possible to connect together all the channels to perform any preselection at chamber level.

The number of BTIs connected to a TRACO is limited from the size of the chip and it is determined by the acceptance requirement. The final design connects four BTIs of the inner Superlayer to twelve BTIs of the outer Superlayer allocated as shown in Figure 2.

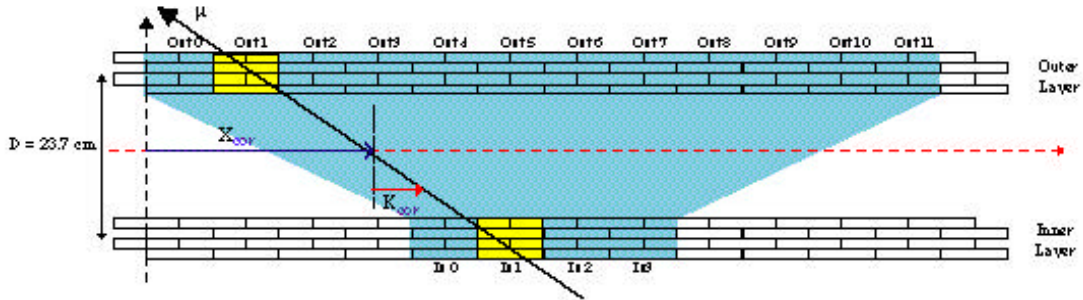


Figure 2 - Track Correlator layout

4. Track Correlator Specifications

The block diagram of the TRACO operations is given in Figure 3. In the following paragraphs we shall describe the TRACO algorithm referring to the flow of this diagram.

4.1 Data paths

In order to allow the identification of two muons inside the same correlator, the TRACO algorithm is applied twice to the data received from the BTI. Therefore inside the TRACO there are two parallel flows delayed by one cycle: the first path computes a First Track, choosing between all the BTI candidates, while the delayed path computes a Second Track from all unused candidates. The programmability of the preferences for the choice of the First Track and the Second Track are completely independent, although in principle we believe that the same criteria should apply.

Inside the full system a further selection is needed in the case that more than one TRACO inside a chamber give a trigger. The communication between the TRACOs and the chamber trigger server to allow this decision is done using a dedicated PREVIEW data bus for each track, in order to minimize the time needed for calculations of the whole trigger chain. A copy of the converted angle (see paragraph 4.3) of one of the candidates chosen for correlation is sent to the Trigger Server according to the programmed H/L and IN/OUT selection flags, before starting any correlation calculation. The Trigger Server selection is based on the quality of the PREVIEW of the various candidates. The preview data is composed by 9 bits: five bits for the module of the converted angle, one bit for the track quality(H/L); one bit identifying First/Second track; one bit identifying Inner/Outer layer; one bit identifying Correlated/Uncorrelated track candidate.

4.2 Input Register (16 x 8bits)

This register receives and latches the data values and the qualification flags from the BTI chip. The TRACO collects the inputs from 16 BTIs (four from the inner layer and twelve from the outer layer).

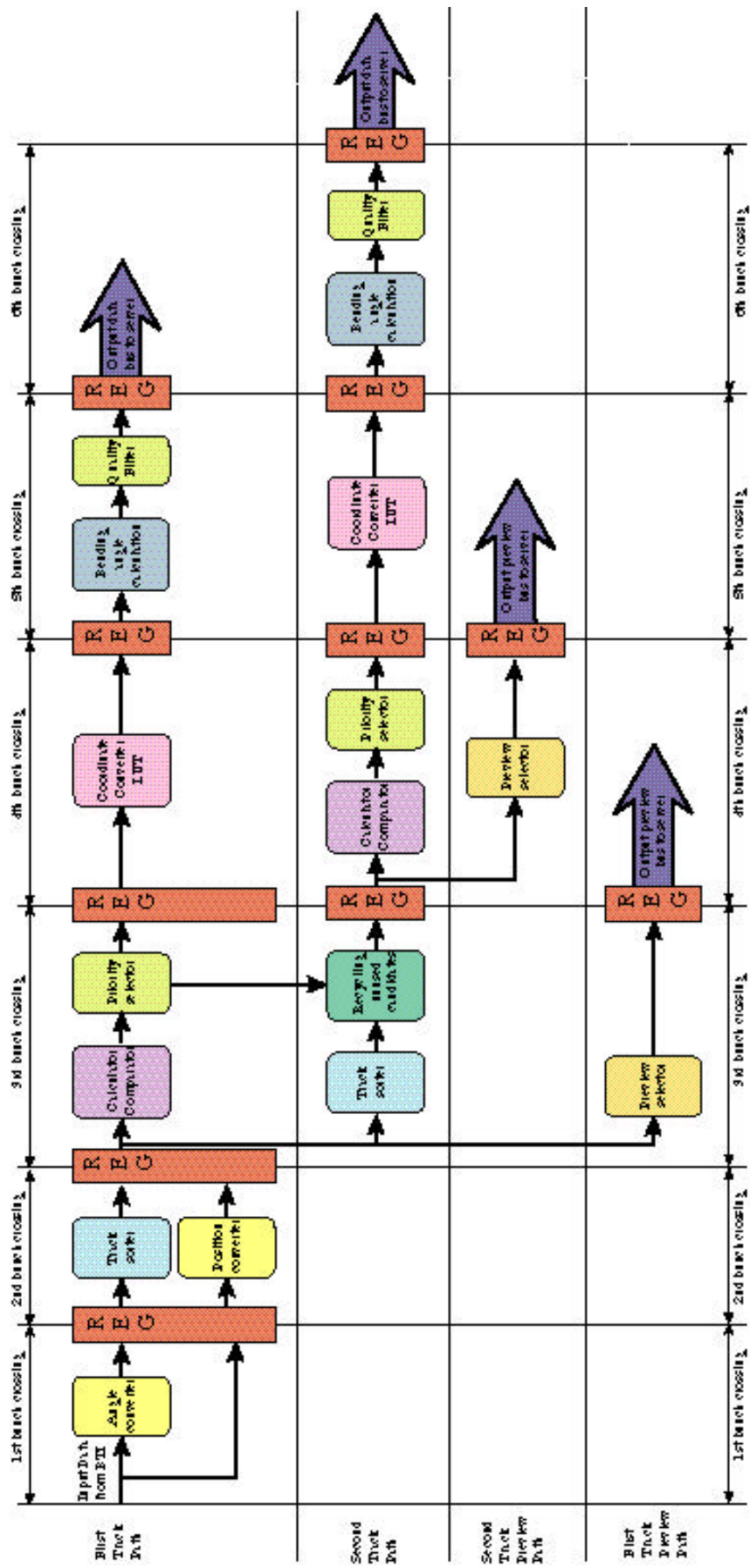


Figure 3 - TRACO Block Diagram

From each BTI the input data bus contains the k-parameter and the position in the BTI coordinate system, multiplexed at 80MHz on the same lines (6 bits wide). Two extra flags are provided: the trigger quality (H/L) and the strobe.

4.3 Angle and position converter

This module receives the k-parameter 6 bits input word from the BTI and converts it into local radial coordinates ($k_{local} = k_{BTI} - RAD - offset$). The RAD parameter is a 6 bits load value, depending on the geographical position of the correlator, i.e. the k-parameter of its center. The offset is a programmed value dependent on drift velocity needed by the BTI for its calculations. The converted angle is used for internal calculations and sent on the Preview bus to the Trigger Server for further track selection.

Each BTI position is converted to TRACO position, offsetting by the appropriate geographical value. An additional Superlayer shift parameter is provided to correct for eventual construction misalignments of the two quadruplets.

4.4 Sorter

This module receives the converted angle and selects the candidate with the smallest angle, i.e. the angle closest to the local radial direction. There is one sorter for the four inner BTIs and another for the twelve outer BTIs, hence the choice is done twice independently on the two ϕ Superlayers.

The sorting operation can be programmed to select the biggest angle instead of the smallest one, and/or to give preference to candidates tagged with the HTRG quality flag.

Two other sorters for the Second Track path exist.

4.5 Calculator and Comparator

This module computes the k-parameter and the position of the correlated candidate. It transforms the inner and outer k-parameter of the two independently selected track segments into the correlator coordinates system and computes the correlated track parameters.

The internal parameters computed for the correlated tracks are:

$$\left\{ \begin{array}{l} k_{COR} = \frac{D}{2} \tan \mathbf{y} = x_{inner} - x_{outer} \\ \\ x_{COR} = \frac{(x_{inner} + x_{outer})}{2} \end{array} \right.$$

The angular resolution of a correlated track candidate is 10mrad for the nominal drift velocity, thus improving the BTI value, while the resolution on the position is unchanged.

A second step compares the three candidates (single inner, single outer, correlated) to set the correlated flag.

If the correlated track fits inside the programmed acceptance window this flag is raised.

4.6 Priority Selector and Preview Selector

This module selects one of the candidates according with some programmed information.

If the correlation was successful the priority selector chooses the correlated candidate and forwards its parameters to the further stages.

If the correlation fails the correlator creates an uncorrelated track following a preference list that includes the parent superlayer (IN/OUT) and the quality bit (H/L) of the two candidate tracks.

If no correlation is possible since there is no candidate in one Superlayer, the existing uncorrelated track is still accepted.

. The trigger quality H/L and the IN/OUT preference selections are chosen according to the following programming mask: high level trigger mask (HTMSK), low level trigger mask (LTMSK), Superlayer mask (SLMSK).

The First Track priority selector or the Second Track priority selector treat the *best* inner candidate, the *best* outer candidate and the correlated candidate considering the trigger quality, the high level trigger mask, the low level trigger mask and the Superlayer mask.

An equivalent priority selector is implemented for the preview path. The PREVIEW priority selector treats the *best* inner and *best* outer candidates, but only considers LTMSK and SLMSK.

A further preference selection can be activated to connect the trigger generated in the transverse view to the triggers generated from the BTIs in the longitudinal view. A programmable coincidence between the two views is foreseen to certify the uncorrelated triggers. In particular, since the noise generated from the BTI algorithm is concentrated in the LTRGs, this coincidence is requested by default for the LTRGs and it is optional for the HTRGs.

The priority selector sends only one candidate towards the output bus, and generates a three bits qualification code as shown in Table 1.

4.7 Recycling unused candidates

Two candidates are needed to fit a correlated track, one from the inner superlayer and another from the outer one. If the correlated track does not satisfy the acceptance value, one of the track candidates selected to try the correlation is forwarded as the First Track choice and the other must be reused for the Second Track calculations. This module performs this recycling task. This feature can be software disabled.

<i>Description</i>	<i>Symbol</i>	<i>Code</i>
HTRG on inner and outer layer	HH	0
HTRG on inner or outer layer and LTRG on inner or outer layer	HL	1
LTRG on inner and outer layer	LL	2
HTRG on outer layer	H _o	3
HTRG on inner layer	H _i	4
LTRG on outer layer	L _o	5
LTRG on inner layer	L _i	6
Null track		7

Table 1 - Codes for output track quality identifier.

4.8 Mixer

The two selected tracks are output on the same bus at consecutive bunch crossing. Therefore it is possible that a Second Track from the previous bunch crossing is computed at the same time of a First Track from the bunch crossing being considered. A First Track choice has always priority on the output bus and therefore overlaps the Second Track from the previous bunch crossing. A flag is activated if an overlap occurs.

4.9 Coordinate converter and bending angle calculation

The internally calculated position and k-parameter are converted, to the chamber reference system: position is transformed to radial angle ϕ and k-parameter to bending angle ϕ_b as defined in Figure 4.

This task is performed with direct access to two programmable look-up tables. The first look-up table is used for conversion of the local correlator position coded in 9 bits to the track radial angle ϕ coded in 12 bits (11 bits plus the sign with 12 bits resolution). The second table performs the conversion from the k-parameter coded in 10 bits to the angle with respect to the normal to the chamber ψ coded in 10 bits (9 bits plus the sign with 9 bits resolution).

A further block performs the computation of the bending angle $\phi_b = \phi - \psi$.

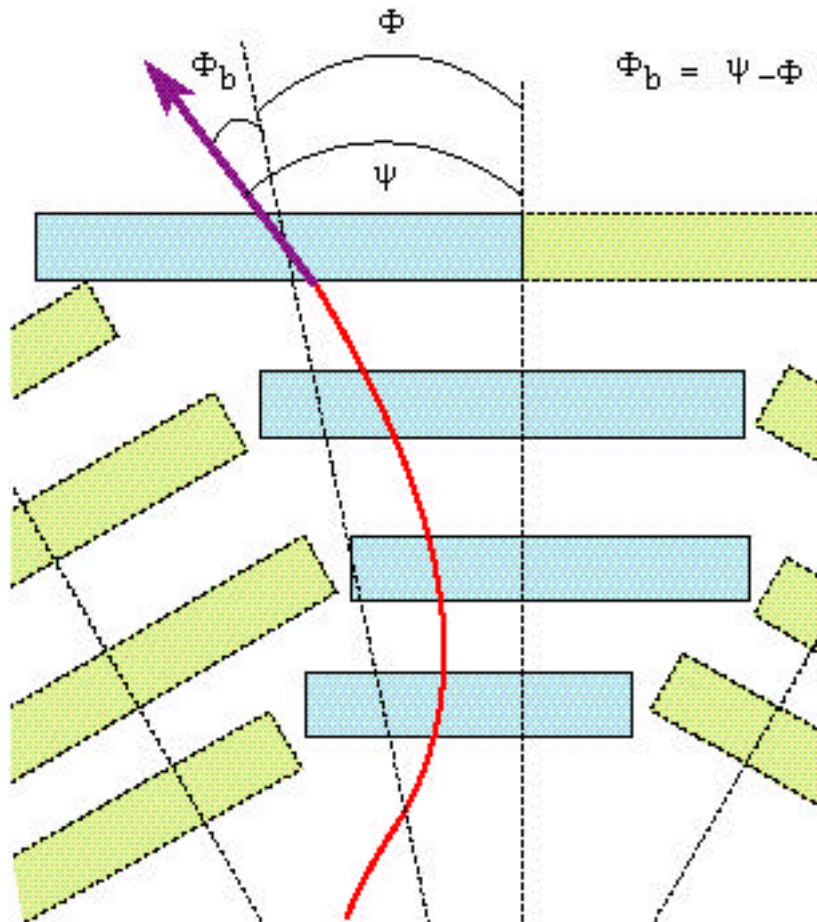


Figure 4 - Definition of the TRACO output parameters.

4.10 Quality filter

Some filtering functions are performed in this block to select the output value driven to the chamber server. These functions include an uncorrelated Low Trigger Suppression and a programmable tolerance window for the bending angle output value. The filters will be discussed in detail in paragraph 5.3.

4.11 Output Data Bus

Data output bus provides one track at each clock cycle, with up to two tracks per bunch crossing at consecutive clock cycles.

The latency for the First Track is five cycles, while Second Tracks are output after six cycles. In case there are two muon tracks at contiguous bunch crossings, the Second Track from bunch crossing n is suppressed and the First Track from bunch crossing $n+1$ is forwarded.

The selected track is output on a bus, using 10 bits for the bending angle and 12 bits for the radial angle and it is accompanied by three quality bits identifying HH, HL, LL, H_i , H_o , L_i , L_o track candidates.

5. Simulation of correlator performance

The correlator algorithm was implemented in the standard CMS software including all the possible programmable choices. Several studies using the full GEANT simulation of the detector were done to see the effect on noise reduction and trigger efficiencies according with the programmed parameters in order to decide their default values.

5.2 Summary of efficiency studies

The efficiency was studied using two samples:

- the first sample consisted of 10000 single muons of $p_T = 100 \text{ GeV}/c$, generated inside the iron in front of one correlator with incident angle $-60^\circ \leq \theta \leq 60^\circ$
- the second sample consisted of 100000 single muons generated from the interaction vertex with $3.5 \text{ GeV}/c \leq p_T \leq 300 \text{ GeV}/c$.

The first sample was used to obtain the general performance of the TRACO, while the second sample provides the actually expected performance of the device inside the CMS detector.

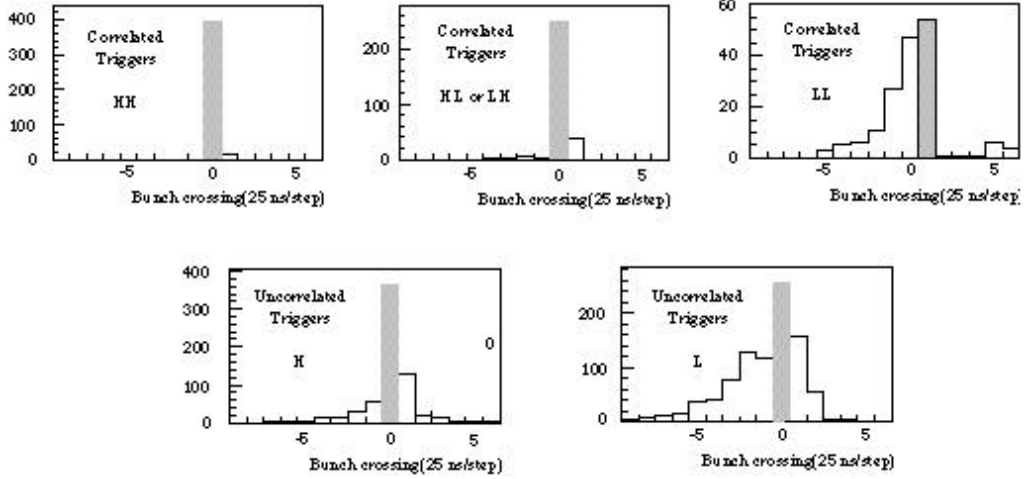


Figure 5 – Time distribution of TRACO triggers, divided by trigger quality.

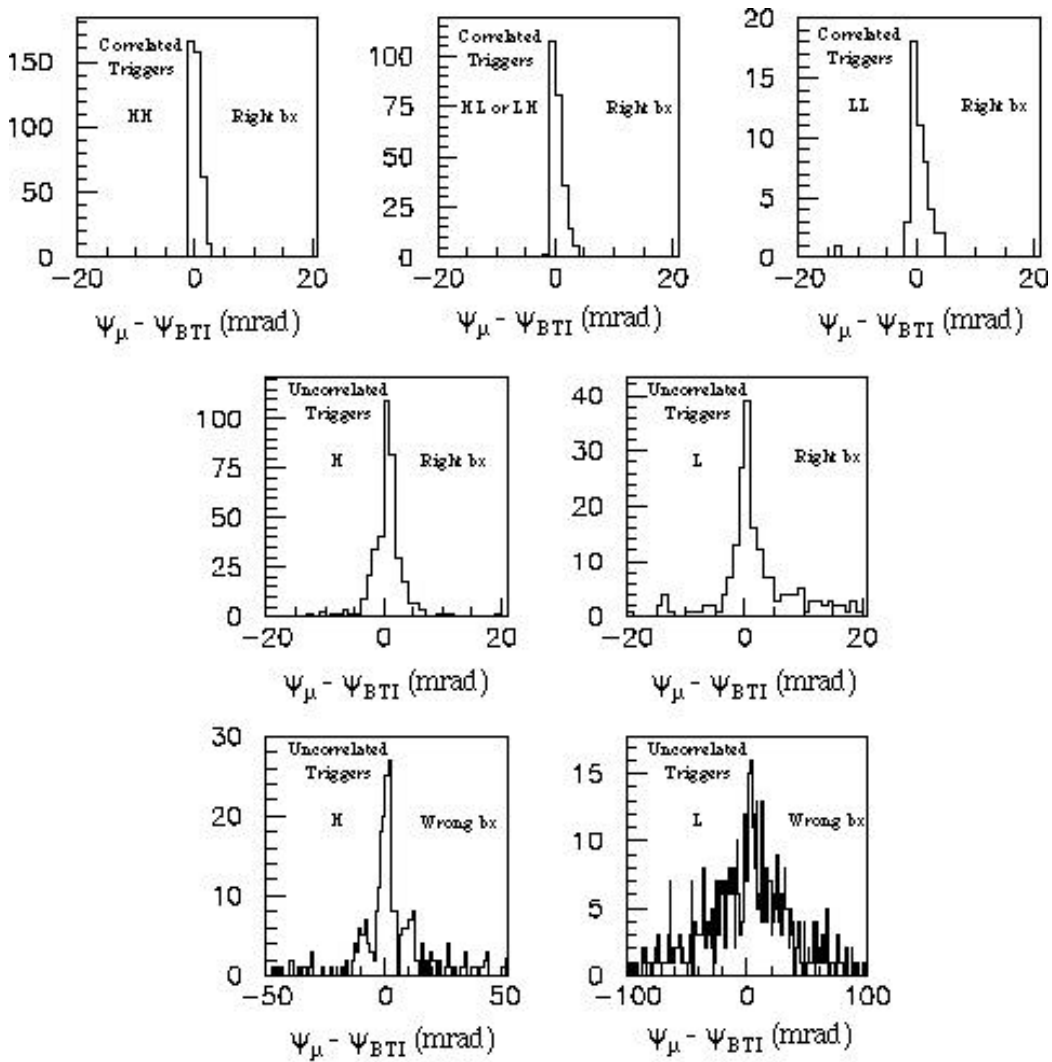


Figure 6 – Difference between the generated and the computed angle for different quality of the triggers. Notice the different scale for the histograms at right bx and the histograms at wrong bx.

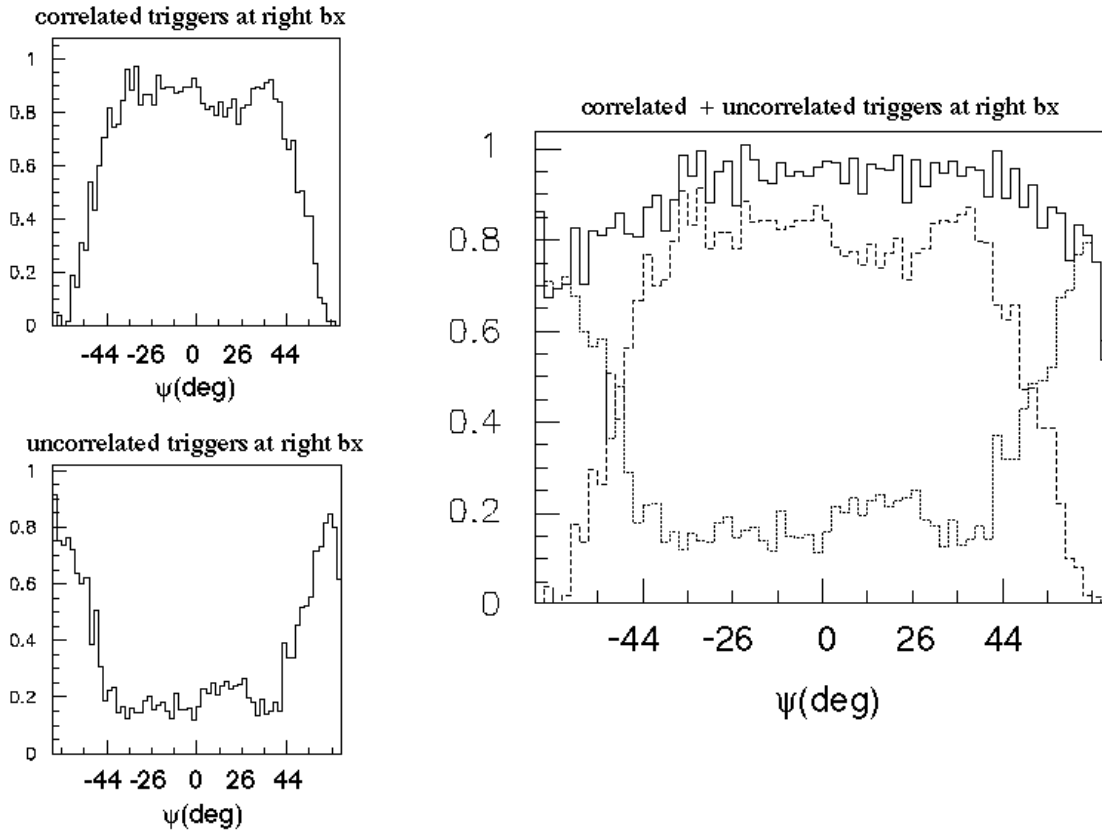


Figure 7- TRACO efficiency as a function of the incident angle (Notice that the scale is not linear).

Figure 5 shows the time distribution of the TRACO triggers, separately for each trigger quality. Correlated triggers containing at least one HTRG segment are quite clean and single uncorrelated HTRGs are reasonably clean. The bunch crossing identification is instead bad for correlated LL and single uncorrelated LTRGs.

Clearly some noise filtering must be provided inside the TRACO to reduce this kind of triggers to an acceptable level. The available filters are discussed in the next paragraphs, but they are all optional, since the importance of the reduction will only be clear on the field.

Figure 6 shows the difference between the computed incidence angle and the actual incidence angle of the muons for different track quality and, only for the uncorrelated triggers, for cases where the determined bunch crossing is the correct or the wrong one.

It is evident from the distribution that the resolution of uncorrelated triggers is worse than the one of correlated triggers. Besides the angle calculated for the uncorrelated LTRGs misidentifying bunch crossing has got a wide range.

Figure 7 shows the efficiency of the TRACO as a function of the angle of incidence: the TRACO has a flat probability (~80%) to correlate within its acceptance 45° range, while outside this range only uncorrelated triggers are available. We do not expect anyway to trigger on tracks with angle larger than 45° .

The performance as a function of the muon momentum was evaluated at the Trigger Server output for three relevant major configurations of the TRACO acting on the uncorrelated LTRGs acceptance:

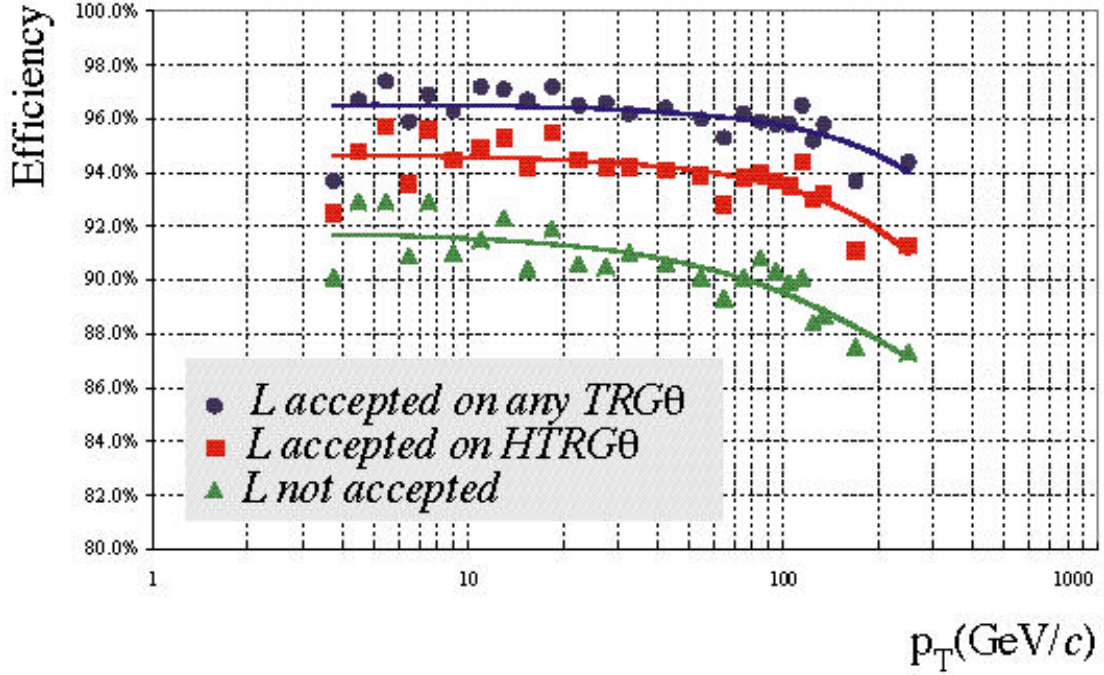


Figure 8 – TRACO efficiency as a function of transverse momentum for the major configurations.

This configurations were:

- L accepted on any q trigger: uncorrelated LTRGs are accepted only if they are confirmed by a BTI trigger of any quality in the θ view. This is supposed to be the standard configuration for data taking
- L accepted on Hq trigger: uncorrelated LTRGs are accepted only if they are confirmed by a BTI trigger of HTRG quality the θ view
- L not accepted : uncorrelated LTRGs are not accepted

The performance for the four muons station, once corrected for station acceptance is the same: therefore we will give only results for station 1.

Figure 8 shows the efficiency, corrected for the muon chambers geometrical acceptance, for the three selected conditions. Before activating the complete suppression of uncorrelated LTRGs there is clearly space for an intermediate step that causes a negligible efficiency loss. But even in the case we are forced to lose uncorrelated LTRGs, the efficiency remains in a sensible range.

In the standard configuration the fraction of events giving triggers only at the correct bunch crossing is slowly decreasing from ~66% at 5 GeV/c to ~60% at 300 GeV/c, while events not triggering at the right bunch crossing are in fact giving triggers only at wrong bunch crossings.

The relative fraction of triggers at the correct bunch crossing divided by track quality is shown in Figure 9 in the standard configuration, showing a roughly constant value.

Since the sample consisted of single muons, the noise markers are the fraction of two tracks per event selected by the TRACO and the quantity of out of time triggers.

Figure 10 reports the fraction of Second Tracks generated by the TRACO selection mechanism and Figure 11 shows the average fraction per generated event of out of time triggers.

Therefore the uncorrelated L suppression, despite generating a large inefficiency, has a very limited effect on the noise reduction.

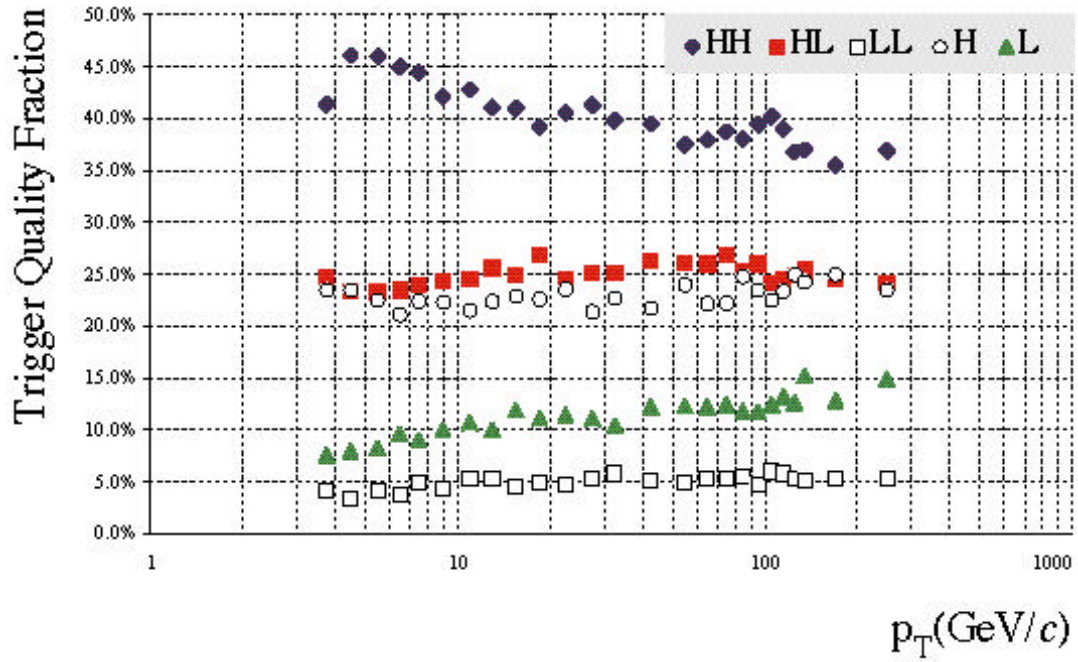


Figure 9 – Relative fraction of triggers divided by quality as function of transverse momentum

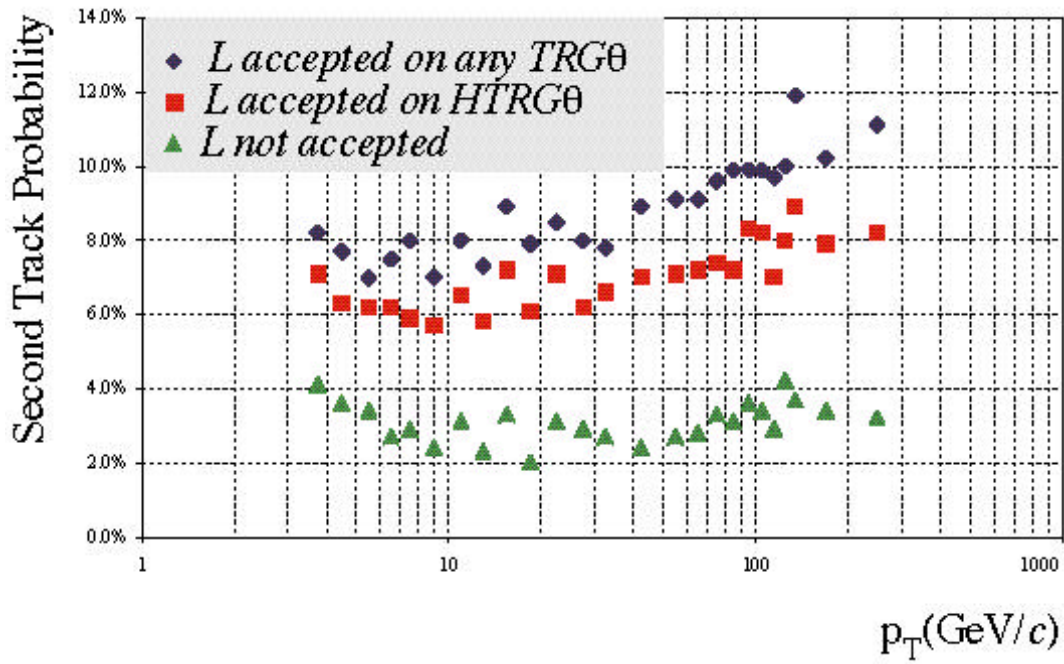


Figure 10 – Fraction of Second Tracks per events as function of transverse momentum for the major configurations

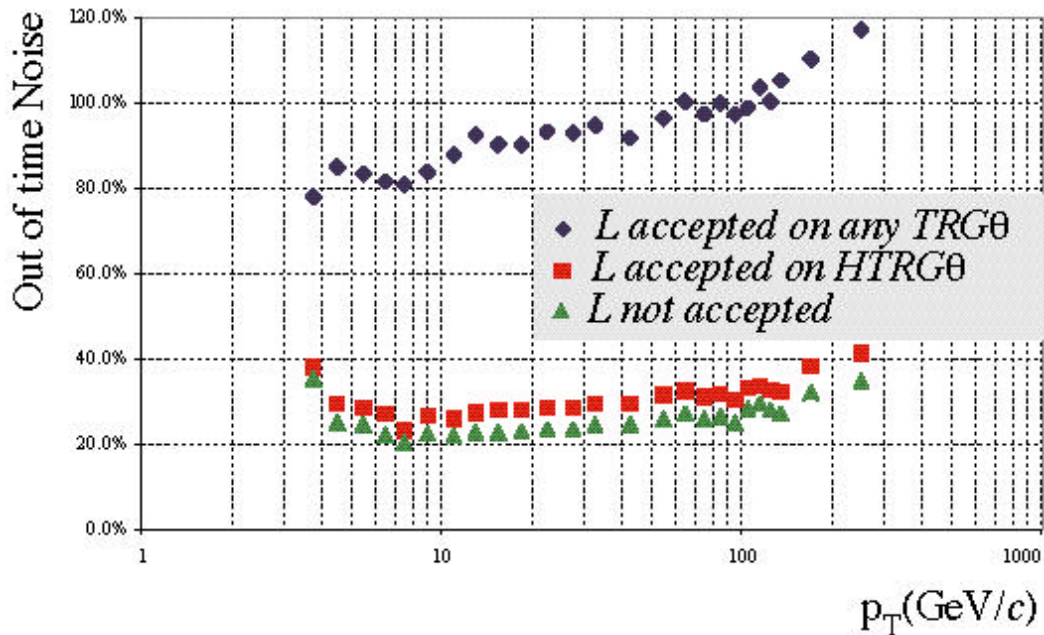


Figure 11 – Fraction of out of time triggers as a function of transverse momentum for the major configurations

5.2 Noise generation mechanisms

The design of the trigger devices was done with the purpose of providing a robust and efficient system. Unfortunately the way to meet these requirements introduces a certain number of redundancies in the system causing an important fraction of false or duplicated triggers.

The BTI trigger algorithm can actually work requiring only three layers of staggered tubes.

The drawback to three layers algorithm is the fact that an inefficiency or a bad measurement on any of the cells becomes an inefficiency or a wrong trigger. The introduction of the fourth layer with the minimal request of an alignment of three out of four hits maximizes the efficiency and minimizes the wrong measurements. But some spurious alignments of three hits can occur at any bunch crossing, depending on the actual track crossing position and in direction.

Most of the bad alignments are generated from the unavoidable left-right ambiguity even at several bunch crossing distance from the alignment of the four hits.

An example of the mechanism is shown in Figure 12: a real track orthogonal to the chamber is displayed and the hit positions are marked with small circles on the track line. The BTI, looking for alignments of at least three hits, is able to find the alignment corresponding to the real track, but other two tracks are detected. These tracks, called *ghost tracks*, correspond to alignments of a mixture of real hits and their mirror images. Indeed the BTI supposing that wire 2 is inefficient and supposing that the signal of wire 4 comes from the right side of the tube, finds a false alignment at time Δt_1 after the right bunch crossing. In the same way, supposing that wire 5 is inefficient, the BTI finds another *ghost track*, formed from the signals of wires 2 and 4 and the mirror image of signal from wire 3, at time Δt_2 before the right bunch crossing.

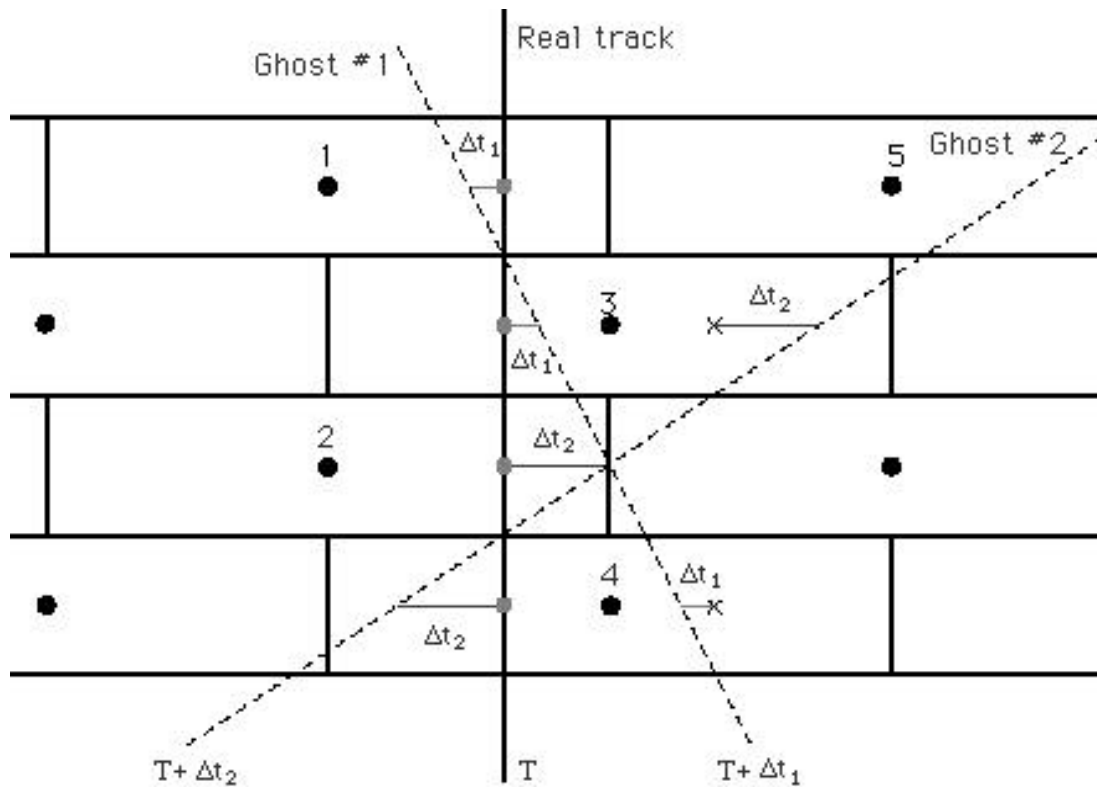


Figure 12 - Illustration of the ghost generation mechanism inside BTI.

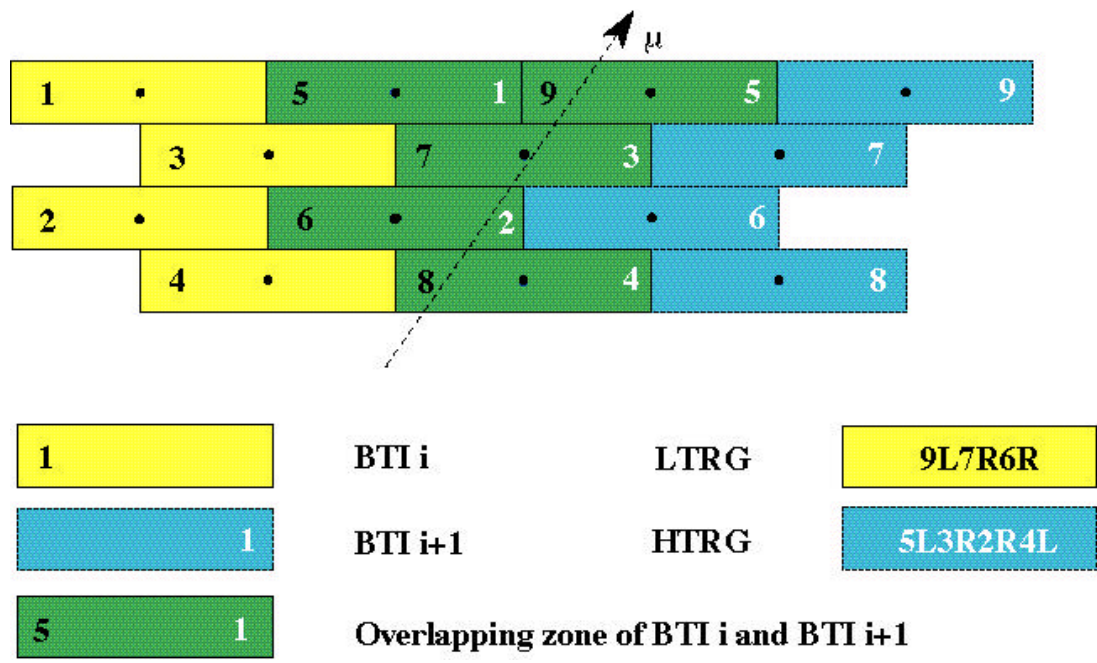


Figure 13 - Illustration of the irreducible redundancies between overlapped BTIs.

Let's call the ghosts generated by this mechanism *noise of type I*.
 Furthermore in order to be fully efficient the trigger system provides some overlapping between adjacent devices: one BTI is overlapped by five cells to its neighbours and BTIs in the outer Superlayer are always assigned to three successive TRACOs.

The overlap between BTIs is foreseen in order to minimize the impact of the loss of one device on the trigger efficiency, since the remaining one can be programmed to partially cover the dead area switching on some redundant patterns.

It is not possible to define a set of completely non-redundant patterns and therefore some of them are available in two consecutive BTIs: in fact there are five redundant patterns generating LTRGs on the devices close to the one generating the HTRG at the same bunch crossing.

In figure 13 we see a case where a valid HTRG pattern in one BTI is also seen as a valid LTRG pattern in the adjacent one.

Therefore the TRACO will have the chance to make a choice between candidate tracks in adjacent BTI's that are images of the same track, carrying exactly the same information. This is not a problem for the First Track sorting, since both are equivalent, but it may result that the TRACO is forwarding the same track twice, with a chance of losing other available candidates. This is called *noise of type II*.

There is third situation (*noise of type III*) that is generating noise candidate tracks. The BTI's in the outer sorter are assigned to three consecutive TRACOs, being in the left, the central or the right group. The BTI data are sent to each TRACO through a dedicated port. Each port is programmed with a different angular acceptance window, depending on the fact that is communicating to the left, central or right group. These tolerance windows are partially superposing: therefore a candidate track falling in the intersection zone, is forwarded from the BTI to more than one TRACO as shown in Figure 14. Hence, as in the case of adjacent BTIs, adjacent TRACOs can forward to the Trigger Server twice the same track. Again this fact may introduce a bias in the Second Track selection at the Server level.

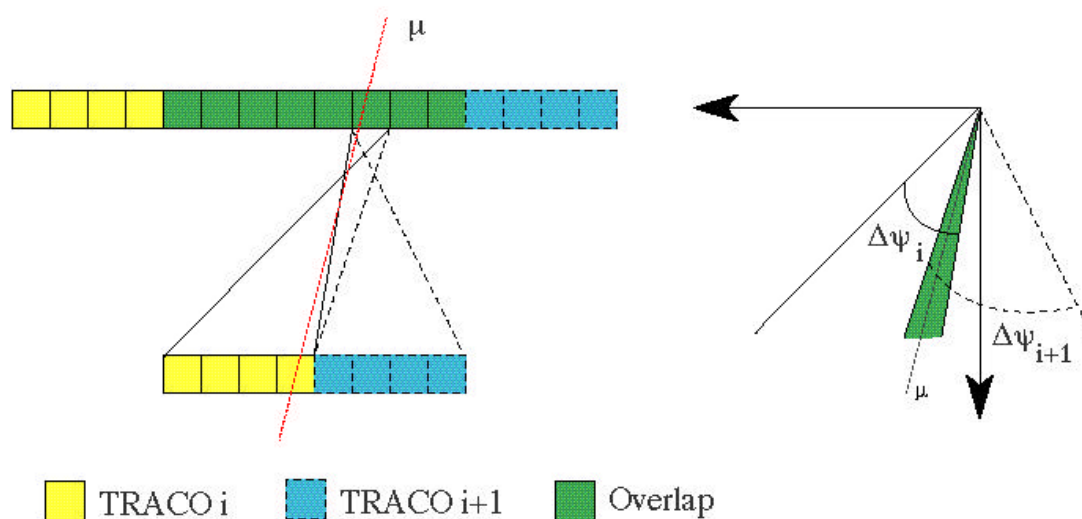


Figure 14 - Illustration of the double track selection due to overlapped TRACOs. The solid lines are the acceptance window of the i -th TRACO and the dashed lines are the acceptance window of the $(i+1)$ -th TRACO. The diagram on the right draws the acceptance windows on the same origin to evidence their intersection (shaded region). A muon falling in this intersection region is assigned to both TRACOs

	Standard	Type I filter on	Type II filter off
Two tracks fraction	6.5%	-	19.4%
Out of time uncorrelated L fraction	53.5%	38.7%	-

Table 2 - Effect of type I and type II noise filters

5.3 Noise reduction studies

We have seen that there is a *temporal* noise, due to left-right ambiguity (type I), that generates ghost tracks at wrong bunch crossings and *spatial* noise caused either by redundancy of the BTI equations (type II) or by the overlap of the BTI acceptance ports (type III), generating copies of the same track.

Some filters have been provided to reduce the overall importance of these effects.

In order to reduce the type I noise we introduced a temporal Low Trigger Suppression: the low quality tracks (L_L, L_o, L_i) are canceled if a HTRG occurred within the neighbouring bunch crossings. It is possible to suppress triggers at bx from -1 to -4 with respect to any HTRG without any latency addition.

Noise of type II and III can affect only the Second Track selection. It is possible to avoid sending twice the same track using a geometrical suppression filter. If a HTRG was selected in the First Track sorting operation, all the LTRGs in the neighbouring BTIs are removed from the Second Track sorting list. This filter, always active, acts on type II noise. A similar procedure, inhibiting Second Track LTRG selection, can be applied to neighbouring TRACOs inside to chamber Trigger Server to remove type III noise. The effect of the application of the filters for type I and II noise is shown in Table 2, compared to a sample of muons at 100 GeV/c in the standard TRACO configuration: the Low Trigger Suppression acts on out of time triggers, while the LTRGs suppression on adjacent BTIs acts on the two tracks fraction.

There is another possible cut to be applied to clean the TRACO output: a programmable tolerance window is implemented for the bending angle. The bending angle for some low

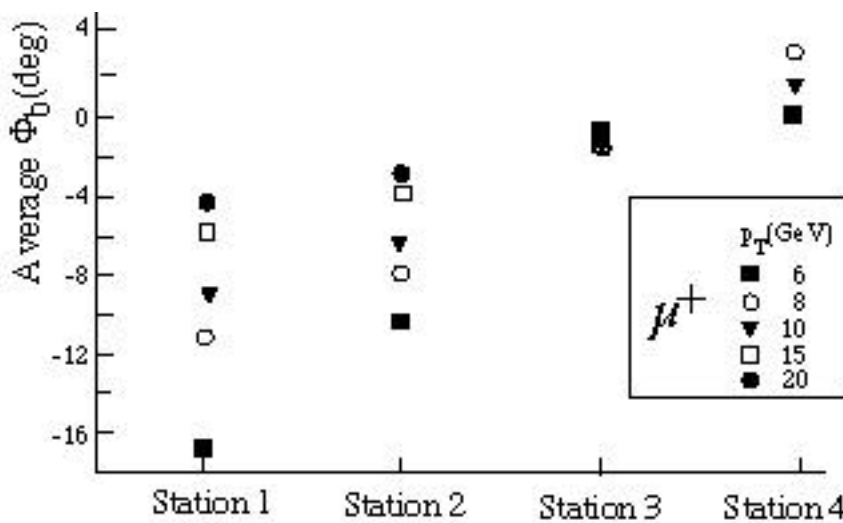


Figure 15 – Average bending angle at the different muon measurement stations for some low transverse momentum muons

Φ_b cut (degrees)	Station 3		Station 4	
	Efficiency (%)	Noise (%)	Efficiency (%)	Noise (%)
51.6	98.0	98.0	98.0	92.6
43.5	97.3	78.0	97.2	75.0
32.3	96.7	65.0	96.8	65.0
17.5	96.4	48.9	95.1	50.7
9.0	94.7	34.2	76.2	30.3

Table 3 – Efficiency and noise for different bending angle acceptance windows in the outer stations.

momentum muons at all the measurement stations is shown in Figure 15. Indeed there is a large spread for the average bending angle values at stations 1 and 2, while the bending angle is close to zero at station 3 and 4.

We cannot safely apply any cut in the first and second station, while a tolerance on the bending angle can be used for station 3 and/or 4.

Table 3 shows the effect of the bending angle cut on efficiency and noise for $p_T = 8\text{GeV}$ muon tracks. The cut is an 8 bits value to be downloaded to the TRACO.

6. Conclusions

Simulations of the TRACK Correlator, needed in the DTBX trigger scheme, show a large improvement of the track resolution and an effective noise reduction.

A large number of user hooks is provided to control the operation flow to reduce the noisy triggers in case of unexpected background.

References

- [1] M. De Giorgi et al., Nuclear Instruments and Methods in Physics Research, A398 (1997), 203.
- [2] G.M. Dallavalle et al., Proceedings of Fourth Workshop on Electronics for LHC experiments, CERN/LHCC/98-36, 294.
- [3] A Kluge and T. Wildscheck, CMS NOTE 1997/091.
A Kluge and T. Wildscheck, CMS NOTE 1997/092.
A Kluge and T. Wildscheck, CMS NOTE 1997/093.
- [4] M. De Giorgi et al., CMS TN 95/01